Hydrothermally Synthesized Ceria with a High Specific Surface Area for Catalytic Conversion of Ethanol to Ethylene

Naotaka OHTAKE[1,4], Yoshiki YAMANE[1], Keizo NAKAGAWA[2,3], Masahiro KATOH[2] and Shigeru SUGIYAMA[2,3]

[1]*Department of Chemical Science and Technology, Tokushima University, 2-1 Minamijosanjima, Tokushima-shi, Tokushima 770-8506, Japan*
[2]*Department of Advanced Materials, Institute of Technology and Science, Tokushima University, 2-1 Minamijosanjima, Tokushima-shi, Tokushima 770-8506, Japan*
[3]*Department of Resource Circulation Engineering, Center for Frontier Research of Engineering, Tokushima University, 2-1 Minamijosanjima, Tokushima-shi, Tokushima 770-8506, Japan*
[4]*Anan Kasei Co. Ltd., 210-51, Ohgata-cho, Anan-shi, Tokushima 774-0022, Japan*

Keywords: Cerium Oxide, Hydrothermal Synthesis, Specific Surface Area, Catalytic Dehydration, Ethanol

Morphological control can be used to improve the catalytic activity of cerium oxide (ceria, CeO_2). In this study, ceria with a high specific surface area was synthesized via the hydrothermal reaction of ceric nitrate and was tested for the catalytic conversion of ethanol to ethylene. As a reference, ceria was also synthesized via a precipitation reaction of cerous nitrate using aqueous ammonia. The Japan reference catalyst JRC-CEO-1 also served as a reference. The specific surface area of the hydrothermally synthesized ceria was as high as that of JRC-CEO-1, but was much higher than that of either reference after calcination at 873 K. Thermogravimetric analysis and IR spectroscopy revealed that the cerias made by hydrothermal and precipitation reactions consisted of high-purity CeO_2, whereas JRC-CEO-1 contained 1.5% decomposable functional groups (OH^-, CO_3^{2-}). For both ethanol conversion and ethylene selectivity in a catalytic dehydration reaction of ethanol, the activity of the hydrothermally developed ceria was higher than that for either reference. The reaction pathway for the dehydration reaction of ethanol over ceria showed that the specific surface area and the basicity of the Lewis basic sites of the ceria were influential properties. The high catalytic activity of the hydrothermally synthesized ceria was derived from its high specific surface area and high-purity CeO_2.

Introduction

Ceria, CeO_2, has characteristic properties that make it a useful material for catalysis applications (Trovarelli *et al.*, 1999; Dai *et al.*, 2012; Bueno-López, 2014; Jain and Maric, 2014), for functional ceramics (Guanming *et al.*, 2007), as a solid electrolyte for fuel cells (Steels, 2000), for use in polishing (Oh *et al.*, 2011), and for use in ultraviolet absorbers (Li *et al.*, 2011). Several approaches have been studied for the development of functional ceria-based materials that could be suitable for these applications. Characteristics such as surface adsorption performance, redox properties (oxygen storage capacity: OSC) associated with the valence change between Ce^{3+} and Ce^{4+}, and a high degree of phase stability have sparked interest in catalysis applications. Efforts to improve the catalytic performance of ceria have included modifications of the crystal structure, crystal morphology, crystal size, and overall crystallinity, as well as modifications to other physical properties, such as the specific surface area, porosity, and particle size distribution. Doping with other elements has also been effective in improving the oxygen ion conductivity (Kumar *et al.*, 2008), surface acidity-basicity (Zhao *et al.*, 2014), specific surface area (Rocchini *et al.*, 2000), and OSC (Ozawa, 2002). The synthesis process and raw materials used must also take into consideration the intended applications of the ceria catalyst. To increase the specific surface area, the formation of small primary particles is preferred. However, primary particles that are too small are readily sintered by heating, which lowers the specific surface area.

To produce ceria with a high specific surface area over a range of temperatures, several synthesis processes have been reported. Bruce *et al.* (1996) synthesized ceria via the precipitation of $(NH_4)_2[Ce(NO_3)_6]$ with ammonium carbonate under a CO_2 gas flow. The specific surface area after calcination at 873 K for 2 h was as high as 200 m^2/g. Kamimura *et al.* (2014) made mesoporous ceria by simple template-free precipitation using $Ce(NO_3)_3$ and NaOH. This oxide had specific surface areas of 200 and 21 m^2/g after drying at 333 K and calcination at 823 K for 10 h, respectively. Nagy and Dékány (2009) synthesized CeO_2 nanoparticles from a toluene/CTAB/$Ce(NO_3)_3$/pentanol system using a microemulsion technique and ammonium hydroxide. The specific surface area of the sample was at most 129 m^2/g. Yang *et al.* (2014) tested the combined sol–gel and solvothermal processing of gels obtained from acet-

Received on May 25, 2015 ; accepted on September 13, 2015
DOI:
Correspondence concerning this article should be addressed to S. Sugiyama (E-mail address: sugiyama@tokushima-u.ac.jp).

aldoximate-modified cerium(IV) *t*-butoxide in the presence of a non-ionic surfactant, Pluronic F127. This process provided ceria with the highest specific surface area of 277 m^2/g, but further calcination at 773 K resulted in a reduction of the specific surface area to 180 m^2/g.

In the present study, ceria with a high specific surface area was synthesized via a hydrothermal process. The synthesis conditions were considered to be suitable for simple and safe mass production using a practical apparatus, only inorganic chemicals, and producing wastewater that could be treated with a simple process. The catalytic performance of the synthesized ceria was tested for the catalytic conversion of ethanol to ethylene by dehydration and the ceria was characterized using various techniques, such as NH_3-TPD, IR, and TG-DTA.

1. Experimental

Ceria was prepared via a hydrothermal reaction. An aqueous solution of ceric nitrate, ($H_x[Ce(NO_3)_{4+x}]$), (Solvay) containing 20 g of CeO_2 was prepared and the final volume was adjusted to 1 L with deionized water. The obtained solution was heated to 393 K, maintained at this temperature for 2 h to obtain a cerium hydroxide suspension, and adjusted to pH 8 with aqueous ammonia. The obtained slurry was separated using a nutsche filter. The cake thus obtained was calcined at 673 K for 10 h under air to obtain ceria powder, which is denoted HSA Ceria. A reference ceria was prepared via the precipitation of cerous nitrate with aqueous ammonia. An aqueous solution of cerous nitrate, ($Ce(NO_3)_3$), (Solvay) containing 200 g of CeO_2, was prepared and the final volume was adjusted to 0.67 L with deionized water. The obtained solution was added to 1.33 L of 3.14 mol/L aqueous ammonia and agitated for 30 min. The obtained slurry was separated using a nutsche filter and washed with deionized water. The cake thus obtained was calcined at 673 K for 10 h under air then ground in a mortar to obtain ceria powder, which is denoted LSA Ceria. A ceria powder (JRC-CEO-1) supplied by the Catalysis Society of Japan was used as a reference.

The specific surface area of the ceria was measured via the BET method using a N_2 isotherm (Macsorb HM model-1220, Mountech Co.). The desorption of ammonia from the catalyst was characterized via temperature-programmed desorption (NH_3-TPD; BELCAT-A-111, Bel Japan Inc.). In NH_3-TPD, a catalyst (50 mg) was heated to 773 K under a He flow (50.0 sccm (standard cubic centimeter per min)), and the temperature was held for 1 h. Then, the catalyst was cooled to 373 K under the He flow and held at 373 K for 10 min. At this temperature, the catalyst was treated with 5% NH_3/He (50.0 sccm) for 30 min. After the treatment, the catalyst was again held under a He flow (50.0 sccm) for 15 min, followed by heating from 373 to 773 K at 10 K/min under a He flow (30.0 sccm). The NH_3 desorbed from the catalyst during the final process was analyzed using a quadrupole mass spectrometer (OmniStar-s, Pfeiffer Vacuum GmbH). The fragment peak at m/z = 16 was used to monitor NH_3. TG-DTA (Thermo plus TG8120, Rigaku Co.) was used for quantitative analysis of the thermally decomposable functional groups contained in the catalyst. A catalyst (10 mg) was heated to 1,273 K at 10 K/min under air with monitoring of the weight changes of the catalyst as well as the temperature difference between the catalyst and the reference alumina pan with temperature. IR spectroscopy was used for qualitative analysis of the thermally decomposable functional groups that were detected via TG analysis. The catalyst was mixed with KBr in a weight ratio of 1:100, and then pelletized. A pellet, 0.1 g, was placed inside an IR cell, heated to 403 K under air, where the temperature was held for 1 h, followed by cooling to ambient temperature. After this treatment, the IR spectra were recorded in the frequency range of 4000–400 cm^{-1}.

Ceria was used in the catalytic dehydration of ethanol to ethylene in a fixed-bed continuous reactor under atmosphere pressure at 673 K. For this reaction, 0.15 g of the catalyst (0.71–1.70 mm) was pretreated at 673 K for 1 h under an O_2 flow (25.0 sccm). The O_2 flow was then switched to He (30.0 sccm) at this temperature. Ethanol (Wako Pure Chemical Industries, Ltd.) was fed into the reactor at a flow rate of 1.7 mL/h. The effluent collected at 0.25, 1.75, 3.00, and 4.50 h was analyzed via gas chromatography (GC-8A, Shimadzu Corp.) using an FID detector. The ethanol conversion and ethylene selectivity for each time point on stream were calculated. Based on the GC analysis, the carbon mass balance in the present study was 100 $\pm$ 10%.

2. Results and Discussion

2.1 Characteristics of hydrothermally synthesized ceria

The transmission electron microscope (TEM) images of the HSA Ceria precursor after drying at 393 K for 10 h (a) and the oxide obtained by calcination of the precursor at 673 K for 10 h under air (b) are shown in **Figure 1**. The precursor consisted of primary particles that were 4–8 nm in size. Faceted structures of some of the primary particles were observed, which indicated that the thermohydrolysis process could be used to synthesize highly crystallite cerium hydroxide. The crystallinity and size of the primary particles seemed to be stable, even after calcination at 673 K under air. The specific surface areas of HSA Ceria obtained by calcination of the precursor at 673 K for 10 h under air and the thus-obtained oxide at 873, 1,073, and 1,173 K for 5 h under air are indicated in **Figure 2**. For comparison, the specific surface areas of the two references are also shown. HSA Ceria had specific surface areas of 139 and 131 m^2/g at 673 and 873 K, respectively. The difference between the specific surface areas was only 8 m^2/g.

JRC-CEO-1 showed a high specific surface area of 149 m^2/g at 673 K, which was dramatically decreased to 66 m^2/g at 873 K. LSA Ceria had low specific surface areas of 55 and 37 m^2/g at 673 and 873 K, respectively. At over 1,073 K, only HSA Ceria maintained a significantly high specific surface area. Based on these results, HSA Ceria was determined to have a high initial specific surface area, as well as high thermal stability.

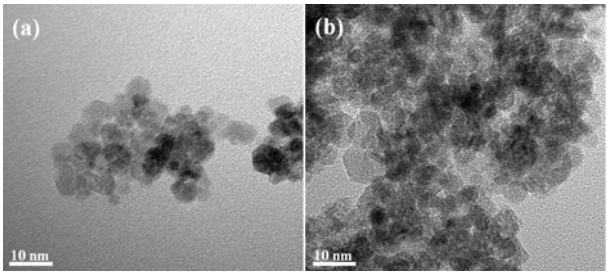

Fig. 1 TEM images of the (a) dried cake and (b) oxide of HSA Ceria

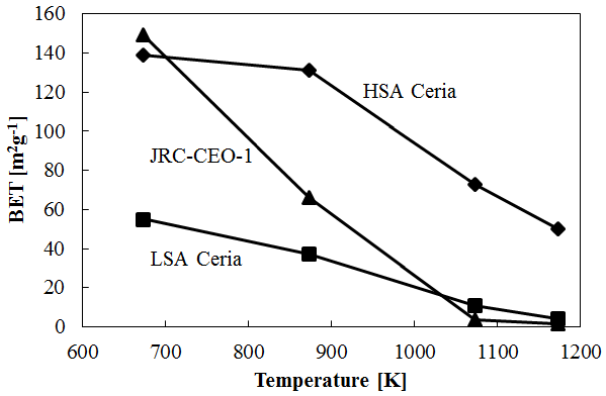

Fig. 2 Specific surface area of HSA Ceria, LSA Ceria and JRC-CEO-1 after calcination at 673, 873, 1,073, and 1,173 K under air

2.2 Catalytic performance of hydrothermally synthesized ceria for the catalytic conversion of ethanol to ethylene

Figure 3 shows the ethanol conversion (a) and ethylene selectivity (b) with time-on-stream over each ceria catalyst. HSA Ceria gave the highest conversion of 29.3% at 0.25 h, and more than 22% of the conversion was maintained on-stream. Both JRC-CEO-1 and LSA Ceria showed conversions that were lower than that of HSA Ceria by 7–9 and 14–19%, respectively. HSA Ceria also had the highest value for ethylene selectivity at 91.3% after 0.25 h on-stream, and approximately 90% of the selectivity was maintained for 4.50 h. JRC-CEO-1 and LSA Ceria showed similar selectivities of between 80 and 85% up to 3.00 h on-stream. However, the selectivity of LSA Ceria quickly decreased to 73.8% at 4.50 h. In the present study, neither diethyl ether nor acetaldehyde was detected on the catalysts. Based on these results, HSA Ceria is a very active catalyst for the conversion reaction of ethanol to ethylene compared with conventional ceria.

2.3 Discussion

The ceria-catalyzed dehydration reaction of ethanol showed a reactivity that varied with the type of ceria catalyst used, as shown in Section 2.2. In this section, the influential properties of the ceria catalysts and the reasons for the high activity of HSA Ceria in the dehydration reaction of ethanol are discussed.

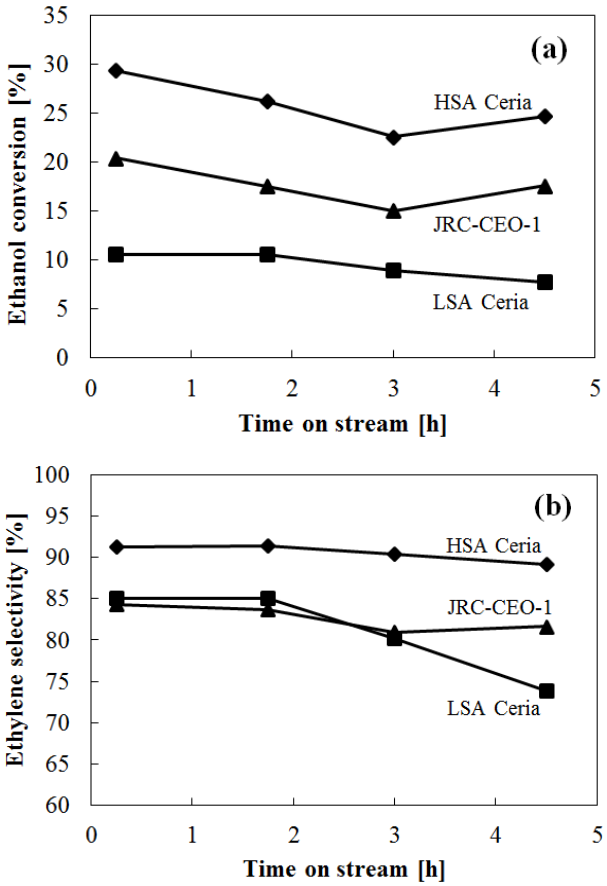

Fig. 3 Ethanol conversion (a) and ethylene selectivity (b) for the catalytic conversion of ethanol to ethylene using a ceria catalyst at 673 K

First, the detailed properties of ceria that could affect the catalytic performance are indicated. **Table 1** summarizes the specific surface areas of each ceria catalyst before and after the catalytic activity test. LSA Ceria showed a much lower specific surface area than that of the other ceria catalysts, which most likely caused its poor catalytic activity. Because JRC-CEO-1 maintained a higher specific surface area than HSA Ceria during the reaction, the specific surface area is likely only one of the key properties of ceria during these reactions.

Because the catalytic reaction occurs on the surface of this catalyst, the surface properties of ceria exert an influence on reactivity. In the dehydration reaction of an

alcohol, the presence of acid sites on the surface of the catalyst is mandatory to initiate the reaction because an acid site can abstract the negatively charged OH^- group.

Table 1 Specific surface area of ceria before and after the activity test for the catalytic conversion of ethanol to ethylene with a ceria catalyst at 673 K

	Specific surface area [m^2g^{-1}]	
	Before activity test	After activity test
HSA Ceria	139	110
JRC-CEO-1	166	137
LSA Ceria	55	56

The acidic properties on the surface of the ceria catalysts were determined via NH_3-TPD, as shown in **Figure 4**. All samples showed one NH_3-desorption peak at approximately 440–473 K, which demonstrated the comparable acid strengths of the acid sites. However, different amounts of adsorbed NH_3 were observed, and the number of acid sites increased in the order LSA Ceria, HSA Ceria, and JRC-CEO-1. This result shows that the catalytic performance was not enhanced when the acid strength of the surface was improved.

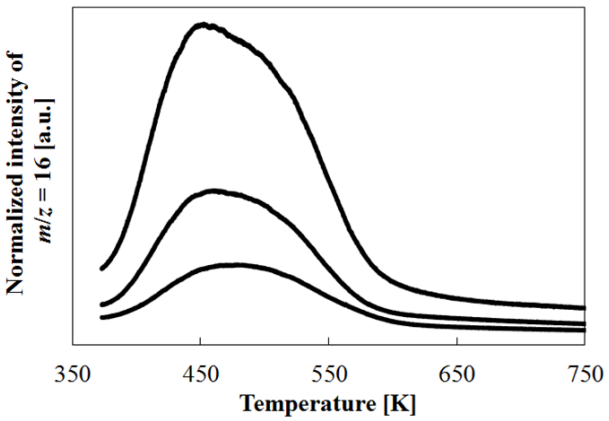

Fig. 4 NH_3-TPD of HSA Ceria, LSA Ceria and JRC-CEO-1

A TG-DTA analysis of each catalyst was performed to determine the presence of any thermally decomposable functional groups. **Figure 5** compares the TG profiles of HSA Ceria before and after the catalytic activity test. The DTA profile of HSA Ceria after the test is also shown. Both materials showed a weight loss that was almost linear until 473 K. This weight loss probably was from the decomposition of physically adsorbed H_2O or CO_2. HSA Ceria after the activity test only showed additional weight loss up to 623 K. As two exothermic peaks appeared between 473 and 623 K in the DTA profile, the weight loss was due to the decomposition of the coke formed during the ethanol dehydration reaction. The much lower coke decomposition temperature on ceria compared with that in the absence of a catalyst results from the OSC property of ceria, which allows the combustion of carbon-containing substances at low temperatures (Bueno-López, 2014). **Figure 6** displays the TG profiles of each catalyst after the catalytic activity test. As shown in Figure 5, the origin of the weight loss up to 623 K was physically adsorbed H_2O, CO_2, or coke. When the TG profile was examined at temperature greater than 623 K, two tendencies were observed for the weight transition. One was the flat or slightly increased weight with temperature detected for LSA Ceria and HSA Ceria, meaning that either no more thermally decomposable functional groups were present or that the oxidation of Ce^{3+} to Ce^{4+} was promoted. The other tendency was the additional weight loss of 1.5% that was observed between 623 and approximately 1,023 K that was only detected for JRC-CEO-1,

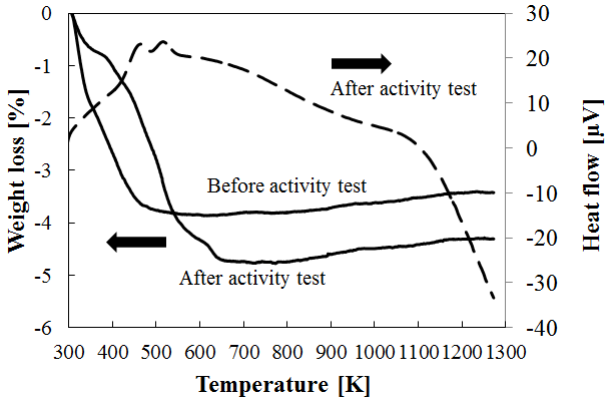

Fig. 5 TG-DTA of HSA Ceria before and after the catalytic activity test. Solid lines are TG profiles and the broken line is the DTA profile

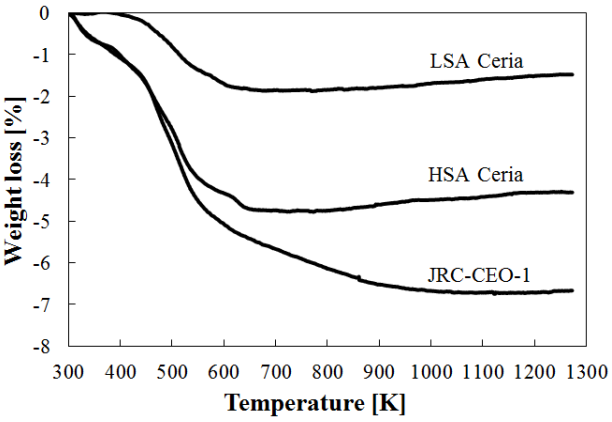

Fig. 6 TG of HSA Ceria, LSA Ceria, and JRC-CEO-1 after the catalytic activity test

which indicated the possible remnants of thermally decomposable functional groups. As both the pretreatment and the main catalytic reaction of the ethanol dehydration test were performed at 673 K, decomposable materials could have remained in JRC-CEO-1 during the catalytic reaction.

An IR analysis was then performed to identify the functional groups on the surface of the ceria catalysts, as shown in **Figure 7**. The IR profile of cerium carbonate (Solvay) is included as a reference. An IR peak in the region of 400–500 cm^{-1} is observed for all the ceria catalysts, which is associated with the Ce-O stretching vibration (Sun *et al.*, 2012). HSA Ceria has no other notable peaks. This means that the surface of HSA Ceria consisted of only Ce cations and oxide ions. LSA Ceria has an IR profile that is similar to that of HSA Ceria, with the exception of a sharp peak at 1,400 cm^{-1} associated with the C-O stretching vibration. The IR spectrum of JRC-CEO-1 shows specific sharp or broad peaks at 850, 1,050, 1,200–1,700, and 3,200–3,600 cm^{-1}. These peaks are ascribed to the stretching vibrations of CO_3^{2-}, Ce-O-C, C=O, and O-H, respectively. As these peaks agree well with the profile of cerium carbonate, JRC-CEO-1 must contain cerium carbonate on the surface. The TG and IR analyses revealed that HSA Ceria and LSA Ceria consisted of pure CeO_2 with no, or very limited amounts of decomposable functional groups, whereas JRC-CEO-1 contained about 1.5% cerium carbonate, which had remained during the catalytic activity test. JRC-CEO-1 may have been prepared by calcination using cerium carbonate as a precursor under air resulting in a few cerium carbonate groups remaining in the oxide.

The existence of a secondary reaction pathway for the dehydration reaction of ethanol using ceria was proposed. There are three possible pathways, denoted by E1, E2, and E1cB, for the catalytic dehydration of alcohols to form alkenes. These pathways depend on the acidity-basicity of the surface of the catalyst that is used and the reaction conditions, such as temperature (Noller and Thomke, 1979; Zaki *et al.*, 1990; Sato *et al.*, 2004; Reddy *et al.*, 2007). When a basic oxide is used as the catalyst, abstraction of the proton from the alcohol is the first step of the reaction. If the proton is a β-H that is bonded to the terminal methyl group, a carbanion is formed, followed by abstraction of the negatively charged hydroxyl group by the acid sites on the catalyst. This reaction is the E1cB mechanism and the corresponding olefin can be preferentially formed. In contrast, if the proton is an α-H or the H of the hydroxyl group, the corresponding aldehyde might be obtained and olefin formation is neither kinetically nor thermodynamically preferred (Beste and Overbury, 2015). In the present study, no aldehyde was obtained and ethylene was formed with high selectivity. In addition, some previous studies revealed that ceria catalysts rupture β-H-C bonds, leading to carbanion formation (Solinas *et al.*, 2003). The ceria catalyst had both weak acid sites and strong base sites, and the most acidic β-H in the alcohol could preferentially adsorb on the basic sites. Therefore, the E1cB route is the most suitable reaction pathway in this study, as shown in the **Figure 8**. The first step of the reaction is the abstraction of the most acidic proton of ethanol by the Lewis base sites, O^{2-}, on the ceria surface to generate a stabilized anion. The lone pair of electrons on the anion then moves to the hydroxyl group, and the negatively charged hydroxyl group is abstracted by the Lewis acid sites, Ce^{4+}, on the catalyst. Following dehydration, the obtained hydrocarbon rearranges into ethylene.

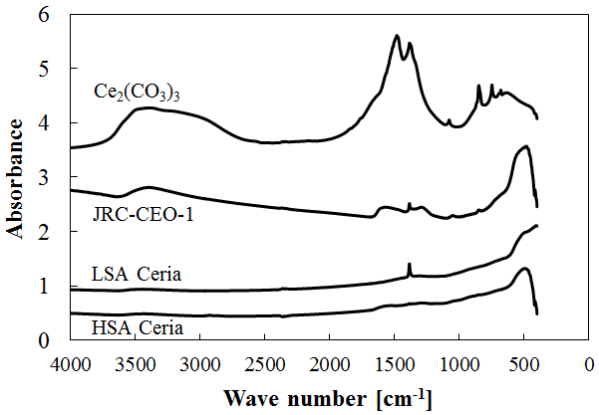

Fig. 7 IR spectra of HSA Ceria, LSA Ceria, and JRC-CEO-1 after the catalytic activity test

The properties of a ceria catalyst that influence the dehydration reaction of ethanol and the beneficial properties of HSA Ceria for the reaction can be summarized as follows. As shown in Figure 8, both Lewis acidity and Lewis basicity on the surface of ceria directly influence the catalytic reactivity. Based on the known ceria properties, the catalytic activity test, and the reaction pathway, higher basicity and a greater number of base sites on the ceria surface promote the first step in the reaction, leading to improvement of the entire dehydration reaction. The specific surface area and the basicity of the oxygen ions are the influential properties. HSA Ceria showed the highest degree of dehydration reactivity because of its high specific surface area and high-purity CeO_2.

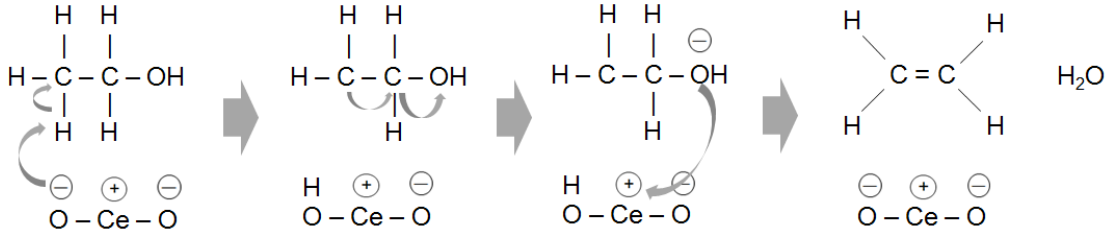

Fig. 8 Possible reaction pathway of the catalytic dehydration of ethanol using ceria

LSA Ceria had similar high-purity CeO_2 (Figure 7), but a lower specific surface area than HSA Ceria. HSA Ceria and LSA Ceria had specific surface areas of 139 and 55 m^2/g, respectively, before the activity test (Table 1). Hence, LSA Ceria only had 40% of the specific surface area of HSA Ceria. In addition, if the acid amount is ascribed as the area under the NH_3-TPD curve in the temperature range of 373–600 K (Figure 4), LSA Ceria showed 46% of the acid amount of HSA Ceria. In the ethanol activity test (Figure 3 (a)), LSA Ceria showed 32–40% of the ethanol conversion of HSA Ceria. In summary, LSA Ceria had comparable acidity and ethanol conversion to that of HSA Ceria if normalized to the specific surface area. In fact, if the acid-base properties of ceria surfaces are similar, ethanol conversion is approximately proportional to the specific surface area. The lower ethylene selectivity of LSA Ceria compared with that of HSA Ceria may be explained by the influence of the space velocity (SV) during the reaction. It is well known that the SV has an impact on the selectivity of a specific product. A high SV may cause a decrease of ethylene selectivity in the catalytic dehydration of ethanol because of the limited reaction time at the active sites on the catalyst (Chen *et al.*, 2007). If the SV is assumed as the flow rate of ethanol divided by the number of active sites on the catalyst in this study, the SV on LSA Ceria is more than twice that of HSA Ceria owing to the difference in the specific surface area. Therefore, the catalytic reaction of the third intermediate in Figure 8 cannot proceed to form ethylene, but by-products might be obtained without the catalytic reaction, leading to lower ethylene selectivity.

JRC-CEO-1 contained 1.5% of cerium carbonate, whereas HSA Ceria had no carbonate. The carbonate is expected to weaken the basicity of the base sites by transition of O^{2-} to OH^- as revealed in the IR spectra (Figure 7). This acidification of the basic sites might inhibit or decrease the reaction rate of β-H abstraction, leading to both lower ethanol conversion and ethylene selectivity.

Table 2 Specific surface area of HSA Ceria and HSA Ceria doped with NH_4HCO_3

	Specific surface area [m^2g^{-1}]	
	Before activity test	After activity test
HSA Ceria	139	110
HSA Ceria + carb.	222	137

To verify the negative impact of cerium carbonate on the dehydration reaction, HSA Ceria containing a small percentage of carbonate was obtained by the same synthesis process as that of HSA Ceria with the addition of 8.2 g of NH_4HCO_3 after adjusting the solution pH to 8. The oxide, which is denoted by HSA Ceria + carb., had a much higher specific surface area, 222 m^2/g, than that of HSA Ceria, as shown in **Table 2**. The specific surface area was decreased to 137 m^2/g after the activity test for the catalytic conversion of ethanol to ethylene at 673 K for 4.5 h, but still maintained a higher value than that of HSA Ceria. A comparison of the TG profiles of HSA Ceria and HSA Ceria + carb. is shown in **Figure 9**. Only HSA Ceria + carb. showed a weight loss above 473 K. As the difference between the weight loss at 1,273 K for HSA Ceria and HSA Ceria + carb. was 4%, HSA Ceria + carb. contained at least 4% of OH^- or CO_3^{2-} decomposable functional groups.

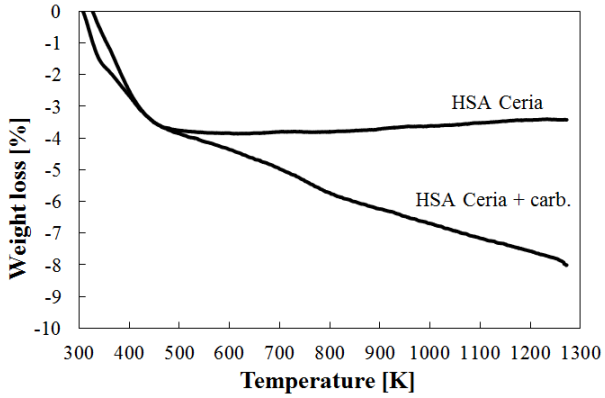

Fig. 9 TG of HSA Ceria and HSA Ceria doped with NH_4HCO_3

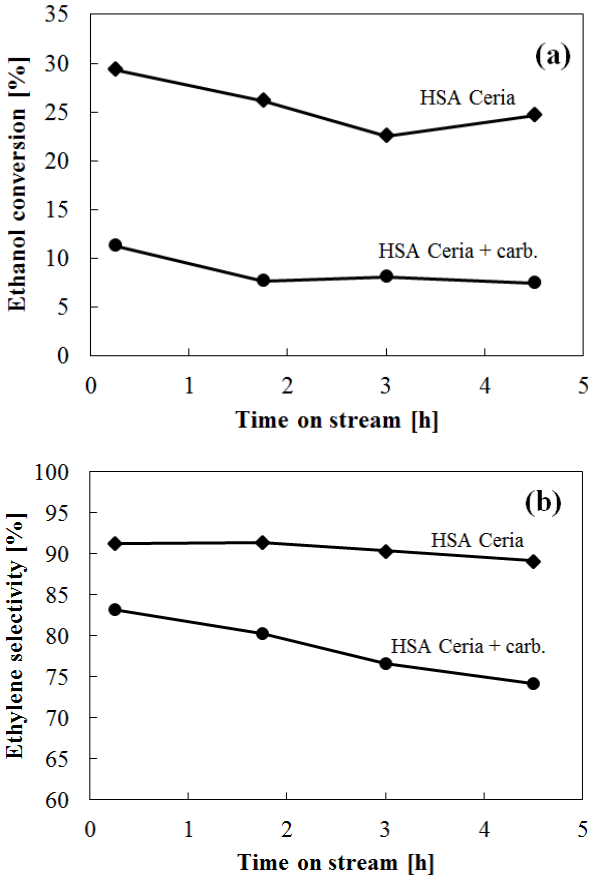

Fig. 10 Ethanol conversion (a) and ethylene selectivity (b) during the catalytic conversion of ethanol to ethylene over HSA Ceria and HSA Ceria doped with NH_4HCO_3

The results for ethanol conversion and ethylene selectivity for the catalytic dehydration reaction of ethanol using HSA Ceria + carb. are shown in **Figure 10**. HSA Ceria + carb. had much lower ethanol conversion and ethylene selectivity than HSA Ceria, with profiles that were similar to that of LSA Ceria (Figure 3). From these results, the presence of a small percentage of cerium carbonate in the ceria catalyst causes dramatic decreases in the catalytic activity during the dehydration reaction of ethanol. Because the use of LSA Ceria and HSA Ceria + carb. led to a similar degree of catalytic activity, the existence of 4% decomposable functional groups of OH^- or CO_3^{2-} and half the specific surface area of ceria had a similar influence on both ethanol conversion and ethylene selectivity. This means not only that ethanol conversion, but also ethylene selectivity, are affected by a complex interaction between specific surface area and purity of ceria.

Both ethanol conversion and ethylene yield tended to decrease with stream-time for all activity tests. A possible reason is deactivation of the catalyst. In a ceria catalyst, a decrease of the specific surface area or the number of the active sites from coke formation on the ceria surface could be suggested. On LSA Ceria, since the specific surface area was similar before and after the activity test (Table 1), whereas the color of the catalyst changed (light yellow to dark gray), the main cause of the gradual decrease of the catalytic activity might be deposition of coke with stream-time. On HSA Ceria and JRC-CEO-1, as the catalytic activity was lower at 4 h than at 0.25 h with a color change of the ceria, coke deposition affected the deactivation of the catalyst. The rapid decline in ethanol conversion from 0.25 h to 3 h seemed to be from an additional decrease of the specific surface area of the ceria.

Conclusion

Ceria with a high specific surface area was prepared via the thermohydrolysis reaction of a ceric nitrate aqueous solution. The initial specific surface area of this ceria was 139 m^2/g, and, even after calcination at 873 K for 5 h, the specific surface area remained at 131 m^2/g. This ceria also consisted of high-purity CeO_2 with no thermally decomposable functional groups. By comparison with conventional ceria, the synthesized ceria showed remarkable catalytic performance during the dehydration of ethanol to ethylene due to its high specific surface area and high- purity CeO_2.

Literature Cited

Beste, A. and S. H. Overbury; "Pathways for Ethanol Dehydrogenation and Dehydration Catalyzed by Ceria (111) and (100) Surfaces," *J. Phys. Chem. C*, **119**, 2447–2455 (2015)

Bruce, L. A., M. Hoang, A. E. Hughes, H. Terence and W. Turney; "Surface Area Control during the Synthesis and Reduction of High Area Ceria Catalyst Supports," *Appl. Catal. A-Gen.*, **134**, 351–362 (1996)

Bueno-López, A.; "Diesel Soot Combustion Ceria Catalysts," *Appl. Catal. B-Environ.*, **146**, 1–11 (2014)

Chen, G., S. Li, F. Jiao and Q. Yuan; "Catalytic Dehydration of Bioethanol to Ethylene over TiO_2/γ-Al_2O_3 Catalysts in Microchannel Reactors," *Catal. Today*, **125**, 111–119 (2007)

Dai, Q., H. Huang, Y. Zhu, W. Deng, S. Bai, X. Wang and G. Lu; "Catalysis Oxidation of 1,2-Dichloroethane and Ethyl Acetate over Ceria Nanocrystals with Well-Defined Crystal Planes," *Appl. Catal. B-Environ.*, **117**–**118**, 360–368 (2012)

Guanming, Q., L. Xikun, Q. Tai, Z. Haitao, Y. Honghao and M. Ruiting; "Application of Rare Earths in Advanced Ceramic Materials," *J. Rare Earths.*, **25**, 281–286 (2007)

Jain, R. and R. Maric; "Synthesis of Nano-Pt onto Ceria Support as Catalyst for Water-Gas Shift Reaction by Reactive Spray Deposition Technology," *Appl. Catal. A-Gen.*, **475**, 461–468 (2014)

Kamimura, Y., M. Shimomura and A. Endo; "Simple Template-Free Synthesis of High Surface Area Mesoporous Ceria and Its New Use as a Potential Adsorbent for Carbon Dioxide Capture," *J. Colloid Interface Sci.*, **436**, 52–62 (2014)

Kumar, V. P., Y. S. Reddy, P. Kistaiah, G. Prasad and C. V. Reddy; "Thermal and Electrical Properties of Rare-Earth Co-Doped Ceria Ceramics," *Mater. Chem. Phys.*, **112**, 711–718 (2008)

Li, J., A. Kalam, A. S. Al-Shihri, Q. M. Su, G. Zhong and G. H. Du; "Monodisperse Ceria Nanospheres: Synthesis, Characterization, Optical Properties, and Applications in Wastewater Treatment," *Mater. Chem. Phys.*, **130**, 1066–1071 (2011)

Nagy, K. and I. Dékány; "Preparation of Nanosize Cerium Oxide Particles on W/O Microemulsions," *Colloids Surf. A Physicochem. Eng. Asp.*, **345**, 31–40 (2009)

Noller, H. and K. Thomke; "Transition States of Catalytic Dehydration and Dehydrogenation of Alcohols," *J. Mol. Catal.*, **6**, 375–392 (1979)

Oh, M-H., J. Nho, S. Cho, J. Lee and R. Singh; "Polishing Behaviors of Ceria Abrasives on Silicon Dioxide and Silicon Nitride CMP," *Powder Technol.*, **206**, 239–245 (2011)

Ozawa, M.; "Ceria and Automotive Catalyst," *Annual Report of the Ceramics Research Laboratory Nagoya Institute of Technology*, **2**, 1–8 (2002)

Reddy, B. M., G. Thrimurthulu, P. Saikia and P. Bharali; "Silica Supported Ceria and Ceria-Zirconia Nanocomposite Oxides for Selective Dehydration of 4-Methylpentan-2-ol," *J. Mol. Catal. A: Chem.*, **275**, 167–173 (2007)

Rocchini, E., A. Trovarelli, J. Llorca, G. W. Graham, W. H. Weber, M. Maciejewski and A. Baiker; "Relationships Between Structural/Morphological Modifications and Oxygen Storage-Redox Behavior of Silica-Doped Ceria," *J. Catal.*, **194**, 461–478 (2000)

Sato, S., R. Takahashi, T. Sodesawa and N. Honda; "Dehydration of Diols Catalyzed by CeO_2," *J. Mol. Catal. A: Chem.*, **221**, 177–183 (2004)

Solinas, V., E. Rombi, I. Ferino, M. G. Cutrufello, G. Colón and J. A. Navío; "Preparation, Characterization and Activity of CeO_2-ZrO_2 Catalysts for Alcohol Dehydration," *J. Mol. Catal. A: Chem.*, **204**–**205**, 629–635 (2003)

Steels, B. C. H.; "Appraisal of $Ce_{1-y}Gd_yO_{2-y/2}$ Electrolytes for IT-SOFC Operation at 500°C," *Solid State Ionics.*, **129**, 95-110 (2000)

Sun, M., G. Zou, S. Xu and X. Wang; "Nonaqueous Synthesis, Characterization and Catalytic Activity of Ceria Nanorods," *Mater. Chem. Phys.*, **134**, 912–920 (2012)

Trovarelli, A., C. Leitenburg, M. Boaro and G. Dolcetti; "The Utilization of Ceria in Industrial Catalysis," *Catal. Today*, **50**, 353–367 (1999)

Yang, J., L. Lukashuk, H. Li, K. Föttinger, G. Rupprechter and U. Schubert; "High Surface Area Ceria for CO Oxidation Prepared from Cerium t-Butoxide by Combined Sol-Gel and Solvothermal Processing," *Catal. Lett.*, **144**, 403–412 (2014)

Zaki, M. I., G. A. M. Hussein, H. A. El-Ammawy, S. A. A. Mansour, J. Polz and H. Knözinger; "Effect of Foreign Ion Additives on Ceria Surface Reactivity Towards Isopropanol Adsorption and

Decomposition: An Infrared Investigation," *J. Mol. Catal.*, **57**, 367–378 (1990)

Zhao, W., Y. Tang, Y. Wan, L. Li, S. Yao, X. Li, J. Gu, Y. Li and J. Shi; "Promotion Effects of SiO_2 or/and Al_2O_3 doped CeO_2/TiO_2 Catalysts for Selective Catalytic Reduction of NO by NH_3," *J. Hazard. Mater.*, **278**, 350–359 (2014)